

Entropy as the driver of chromosome segregation

Suckjoon Jun and Andrew Wright

Abstract | We present a new physical biology approach to understanding the relationship between the organization and segregation of bacterial chromosomes. We posit that replicated *Escherichia coli* daughter strands will spontaneously demix as a result of entropic forces, despite their strong confinement within the cell; in other words, we propose that entropy can act as a primordial physical force which drives chromosome segregation under the right physical conditions. Furthermore, proteins implicated in the regulation of chromosome structure and segregation may in fact function primarily in supporting such an entropy-driven segregation mechanism by regulating the physical state of chromosomes. We conclude that bacterial chromosome segregation is best understood in terms of spontaneous demixing of daughter strands. Our concept may also have important implications for chromosome segregation in eukaryotes, in which spindle-dependent chromosome movement follows an extended period of sister chromatid demixing and compaction.

In bacteria, the two defining processes of the cell cycle, chromosome replication and segregation, progress hand in hand. The roles of the enzymes and proteins involved in chromosome replication have been well studied in *Escherichia coli*¹. Chromosome segregation, on the other hand, was described by Murray and Hunt in 1993 (REF. 2) as “among the most mysterious” events during the bacterial cell cycle, and its basic mechanism remains elusive.

At the heart of the problem is the fact that the stretched length of a chromosome is at least 1,000 times as long as the cell, thus chromosomes — be they eukaryotic or bacterial — experience a strong confinement inside a cell, and individual proteins can probe only a fraction of the chromosome owing to their own small sizes. It is this immense difference in scale between proteins and chromosomes that makes it difficult to understand how the local actions of specific proteins can result in the global changes that take place during the organization, decatenation and segregation of the bulk chromosomes. This is particularly pertinent to proteins like type II topoisomerases or the SMC (structural maintenance of chromosomes) proteins. Type II topoisomerases are known to be crucial for chromosome segregation in both bacteria and eukaryotes³, but how do they know whether two strands of DNA belong to the same or different chromosomes? Similarly, it has

been proposed that DNA condensation by SMC proteins contributes to chromosome segregation^{4,5}, but it is not clear why mixed polymers will not become even more intermingled when condensed by such proteins. These examples stress the importance of directionality of the guiding forces for the action of proteins in the organization and segregation of chromosomes.

Here, we propose a physical biology framework for understanding not only how the global physical properties of the chromosome provide directionality for the action of proteins such as topoisomerases, but also which of these physical properties should be influenced by proteins in order to establish global organization and segregation of the chromosome. Specifically, we put forward the theory that conformational entropy is a major guiding force for segregation of chromosome bulk, and that the proteins previously identified as segregation factors in fact function to create the right physical conditions for entropy-driven chromosome segregation.

In the first part of this Opinion article, we consider when entropy will drive segregation and then present a physical model of the bacterial chromosome to explain chromosome segregation in *E. coli*. A corollary of our model is that accurate segregation of smaller DNA circles such as plasmids cannot rely on entropic force alone, unlike chromosomes, but require active partitioning

systems. Fully consistent with our proposal, cytoskeleton-based mechanisms have been described in detail for the segregation of low-copy-number plasmids⁶, whereas evidence is lacking for a chromosome segregation mechanism that is purely cytoskeleton based. In the second part of this Opinion article, we critically examine the protein-based DNA segregation models and explain how they can be understood in the context of the entropy model. Finally, we compare chromosome segregation in bacteria and eukaryotes, emphasizing the common physical principles.

Entropy can drive segregation

When will conformational entropy drive segregation? As we illustrate in BOX 1 and in [Supplementary information S1](#) (movie) and [Supplementary information S2](#) (movie), polymers confined in a box can actively segregate, whereas disconnected but otherwise physically identical particles always mix. This can be understood in a two-dimensional example by imagining a long polymer chain as a random walk that cannot cross its own path (a so-called ‘self-avoiding random walk’). More specifically, consider a long chain on a paper surface that cannot cross itself, surrounded by a tightly confining box. Now, draw a second chain in the same box but without allowing the chains to cross. Finding overlapping (intermixed) but self-avoiding conformations is a challenge. The reason is that — using the terminology of polymer physics — the overlapping chains have fewer conformational degrees of freedom, or less conformational entropy, than the ones that are completely separated. Thus, entropic forces can actively segregate mixed polymers from one another.

Conformational entropy can be measured quantitatively using the concept of a ‘blob’ (REF. 7). A blob is the largest unit of a polymer, under a particular set of conditions, that shows the characteristics of an unperturbed self-avoiding chain, even in the presence of external forces such as compression or pulling. If the chromosome some has internal structures within which DNA motions or dynamics influence one another, these structures can be measured experimentally and considered to be a blob as well ([Supplementary information S3](#) (box)). A blob is also the basic unit of free energy stored in a strongly deformed polymer. Compressing or stretching an unperturbed chain requires that the polymer’s tendency to go back to its natural size — which is $(\text{contour length})^{3/5}$, so much smaller than its fully stretched length — must be overcome. Thus, a stretched chain

stores free energy like an ‘entropic spring’ (REF. 8), and this entropic spring consists of a string of blobs (BOX 2). For the same reason, strongly confined chains behave like a loaded entropic spring. Indeed, as we describe below, we view the bacterial chromosome as a loaded entropic spring of blobs, in which each blob is a structural unit of the chromosome and consists of supercoiled DNA stabilized by DNA-binding proteins⁹, thus storing the free energy produced by the DNA–protein interactions (such as depletion interactions, as illustrated in BOX 1, DNA–gyrase interactions that generate torsion, and binding of SMC proteins for DNA condensation).

The size of the blob simultaneously influences the organization of two chains (segregation versus mixing) and their conformation (ordered versus random) in a closed confinement. To understand this, consider two chains trapped in a cylindrical pore closed by two pistons, as illustrated in FIG. 1a. When the chain concentration is low, the two chains are well separated, as their mixing is entropically costly (because blobs repel one another). As the pistons decrease the volume of the cylinder and the pressure builds up, the two chains become more compressed and, thus, their free energy increases — imagine an ideal gas being compressed. Free energy is directly proportional to the number of blobs, so compressed chains have more blobs and, accordingly, these are smaller (see *Supplementary information S4* (box)).

At the beginning of the compression process, the two chains will repel each other — because the large blobs forming the chains repel one another — while maintaining their linearly ordered conformation inside the pore. However, this segregated state cannot last indefinitely. Once the blobs become substantially smaller than the width of the cylinder, the chain gains more conformational freedom by giving up its linear organization and taking on a random conformation. In other words, two transitions occur simultaneously as compression continues: from segregation to mixing, and from linear organizations to random conformations.

What will happen if we change the shape of the confinement, keeping its volume constant? (Because there is a constant chain concentration, owing to the constant volume, there will be no change in confinement free energy and therefore no change in the number and size of blobs.) A general rule is: the longer the box, the better the segregation and the stronger the linear ordering of the

Box 1 | Entropy measures the degrees of freedom, not disorder, of the system

In his influential book, *What is Life?*⁵⁰, Schrödinger asserted that a living being reaches thermodynamic equilibrium only on its death. Defining entropy as a measure of ‘disorder’ in the last chapter, he struggled to explain how order (life) can be achieved from disorder. However, this association of life with minimal entropy can be misleading. Molecular dynamics simulations (see the figure, part a, and *Supplementary information S1* (movie)) can be carried out for a long rectangular box containing two species of particles in equilibrium (blue and red) that are initially separated by a wall. As the wall is removed from the system, the two species start to mix. The driving force of this process is the well-known ‘entropy of mixing’.

Entropy, however, is more subtle than a simple measure of disorder. To see this, let us start with the mixed state of the particles and connect those of the same species, creating two long linear chains, one blue and one red (see the figure, part a). Another important condition is the excluded-volume interaction between the particles. The reader is encouraged to perform this simple computer simulation, and he or she will see that the two chains demix; that is, ‘order’ emerges out of disorder (see *Supplementary information S2* (movie)).

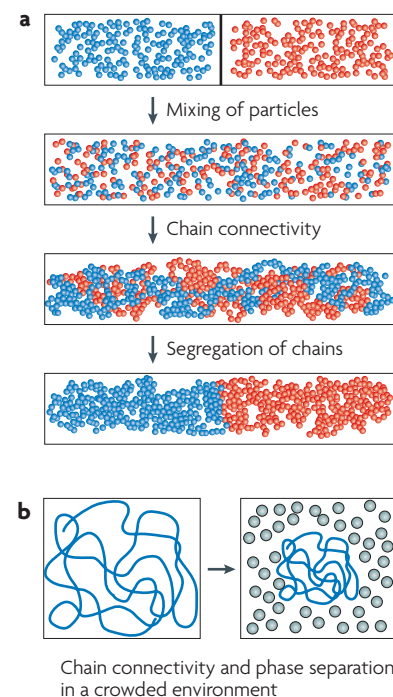
Another example of order arising out of disorder is the phase separation of a long polymeric chain (for example, double-stranded DNA) embedded in a solution of small molecules (for example, globular proteins), in which the small molecules are depleted from the long chain because of their excluded volume (see the figure, part b). The result of this entropic interaction is the compaction of the long-chain molecule.

These are some of the many examples of entropy leading to order that we have come across since Schrödinger’s time*. They clarify what entropy really measures — namely, the degrees of freedom of the system (rather than the ‘disorder’ of the system). These two examples also point out the importance of chain connectivity, a keyword in polymer physics. This emergence of order from disorder owing to entropy arising from chain connectivity is our starting point for understanding chromosome organization and segregation in bacteria.

*Note that polymer physics was still in its infant stage during Schrödinger’s time. For example, Flory’s magnum opus, *Principles of Polymer Chemistry*⁵¹, appeared almost 10 years after Schrödinger’s *What is Life?*⁵⁰.

confined chains (see *Supplementary information S4* (box); see below for segregation in a round cell).

We can translate the above qualitative descriptions into a rigorous phase diagram that can tell us the ‘segregability’ of two confined chains in a three-dimensional box of a given size and shape. In other words, it tells us how well two chains will segregate in a particular environment owing to entropic forces (FIG. 1b). Briefly, regime I in the phase diagram describes polymers in dilute solution without any confinement, such as an isolated, free-floating DNA in dilute solution. Regime II describes a long cylindrical confinement in which the confined linearly elongated chains are well separated from one another. Regimes III, IV and V describe a closed box in which polymers are under moderate to strong confinement of varying geometries, from rod shapes to flat spheres



Chain connectivity and phase separation in a crowded environment

via round shapes that are relevant to most bacteria. Regime VI describes a slab-like geometry. See *Supplementary information S4* (box) for the full quantitative descriptions.

Application to Escherichia coli chromosomes and plasmids. To determine where *E. coli* fits on this phase diagram, we need a coarse-grained, physical model of a bacterial chromosome (summarized in FIG. 2a), which is a string of structural units (blobs) that are closely packed in the nucleoid volume. Three parameters characterize our

Glossary

Contour length

The length of the polymer at maximum extension.

Ideal gas

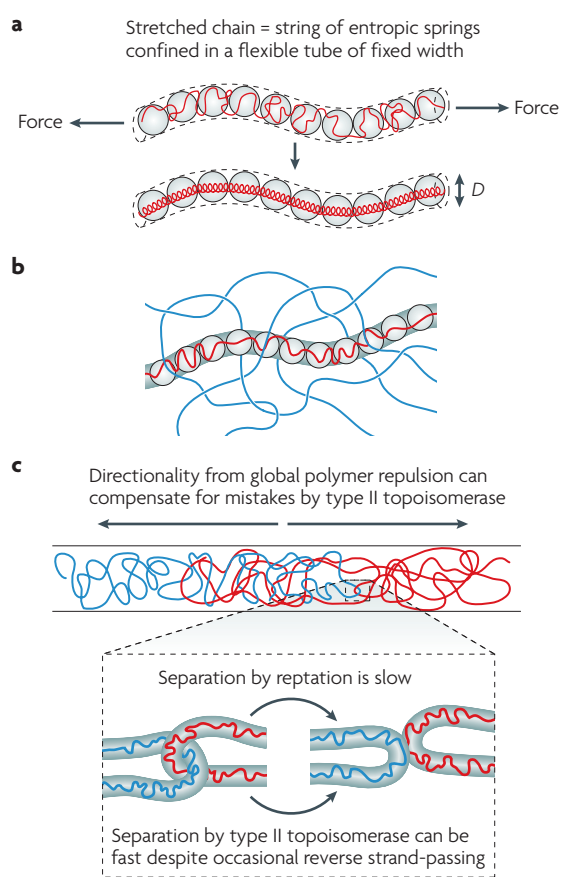
A theoretical gas consisting of randomly-moving, non-interacting point particles.

Box 2 | Chain molecules in strong confinement or at high concentrations

The effect of a cylindrical confinement on a chain is equivalent to applying a tension, which pulls and stretches the long molecule (see the figure, part **a**). In polymer physics, the stretched chain is described as a series of entropic springs (or ‘blobs’), the size of which is determined by the width of the tube. There is a linear relationship between the total contour length of the chain and the total number of blobs, and the free energy stored in the chain is directly proportional to the number of blobs. In other words, a blob is also a basic unit of free energy stored in a polymer and has a thermal energy of $k_B T$ (where T is the room temperature (~300 Kelvin) and k_B is the Boltzmann constant (2 cal per mol K) regardless of its physical size^{52,53} (for comparison, ATP hydrolysis releases ~12 $k_B T$ of energy, and a hydrogen bond is several $k_B T$). In other words, blobs can have different sizes but the same free energy, as long as the self-avoidance condition is met.

When the concentration of the chain is very high, transverse motions of a chain segment embedded in the meshwork of polymers is hindered. In this case, the polymer motion is best understood as sliding in a conceptual tube embedded in a polymer meshwork, also known as ‘reptation’ (see the figure, part **b**). Reptation is slow; it takes much longer to travel the same absolute distance by reptation in a meshwork than by diffusion in the absence of the meshwork, and the difference between the rates increases in proportion to the length of the chain itself.

Chain connectivity and excluded-volume interactions provide directionality for the segregation of intermingled chains⁵⁴ (see the figure, part **c**). Type II topoisomerases do not need to provide or know the directionality. By occasional random strand-passing, these enzymes can accelerate the kinetics of chromosome segregation because reptation is a much slower process (see the figure, part **c**). However, too high a concentration of topoisomerase means that the two chains will not know their directionality, because the excluded-volume interaction between the chains and the enzyme effectively vanishes (by virtue of the high concentration of the enzyme) and the forward and reverse topoisomerase reactions will cancel each other out. We thus predict that there will be an optimal range of type II topoisomerase concentrations at which chromosome segregation is fastest, because the entropy-driven directionality and topoisomerase-dependent ‘free pass’ are in balance.



physical model of the *E. coli* nucleoid: the size of the structural unit (also called the correlation length; ξ); the Flory radius of gyration (R_F) of the isolated nucleoid (namely, the diameter of the fully expanded nucleoid released from the lysed cell); and the length and width (L and D) of the nucleoid inside the cell. The most important parameter is ξ , which can be measured as described in Supplementary information S3 (box).

Experimentally, *E. coli* str. B/r H266 is the only organism for which these parameters have been measured^{10,11} (see BOX 2 and Supplementary information S3 (box)). They are: $D = 0.24 \mu\text{m}$, $L = 1.39 \mu\text{m}$, $R_F = 3.3 \mu\text{m}$; and $\xi = 87 \text{ nm}$. Thus, *E. coli* str. B/r H266 belongs to regime III, in which the strongly compressed individual chromosomes gain maximum conformational entropy when they remain segregated and linearly ordered (FIG. 1c; see Supplementary information S4 (box)). Similarly, our phase diagram can be used to make a prediction for other bacteria such as *Vibrio cholerae* (which has two chromosomes), *Bacillus subtilis* and *Caulobacter crescentus*. At present, neither the size of

the isolated nucleoid nor the size of the structural unit have been measured for these organisms, although we expect *B. subtilis* and *C. crescentus* to belong to regime III, considering that both organisms have similar cell dimensions and genome sizes to *E. coli*. Future studies are needed to measure ξ for the nucleoids in these organisms, perhaps using fluorescence correlation spectroscopy techniques similar to those used in REF. 11 (explained in Supplementary information S3 (box)) in order to fully test our predictions.

The next question concerns plasmid segregation in bacteria. Note that plasmids make little contribution to the amount of DNA in the cell because of their small sizes. Indeed, R_F for plasmids is typically one-tenth of the R_F value for the chromosome. This separates the plasmids from the chromosomes by one order of magnitude along the diagonal line between the two axes in the phase diagram (FIG. 1c; see Supplementary information S4 (box)). As a result, plasmids belong to the lower part of regime V in the phase diagram, in which polymers are

not confined and the entropic repulsion between them is weak. In the absence of any specific interactions with the chromosome (such as ‘hitchhiking’), or without dedicated segregation machinery, plasmids will distribute randomly inside the cell because of their small sizes. Indeed, recent experimental results from studies of the high mobility and random distribution of the RK2 plasmid, which lacks a partitioning system, are fully consistent with our prediction¹².

Segregation in round cells. Perfect symmetry of cell shape means that the confined chains do not have any preferred conformations between mixing and segregation, although their global reorganization is readily achieved¹³. Few data are available about chromosome organization in spherical bacteria, so we can only speculate about possible contributing factors to segregation. We think that supercoiling is the most important factor, as it gives rise to the branched structure of the bacterial chromosome¹⁴. We did not take into account the topological complexity of the polymer

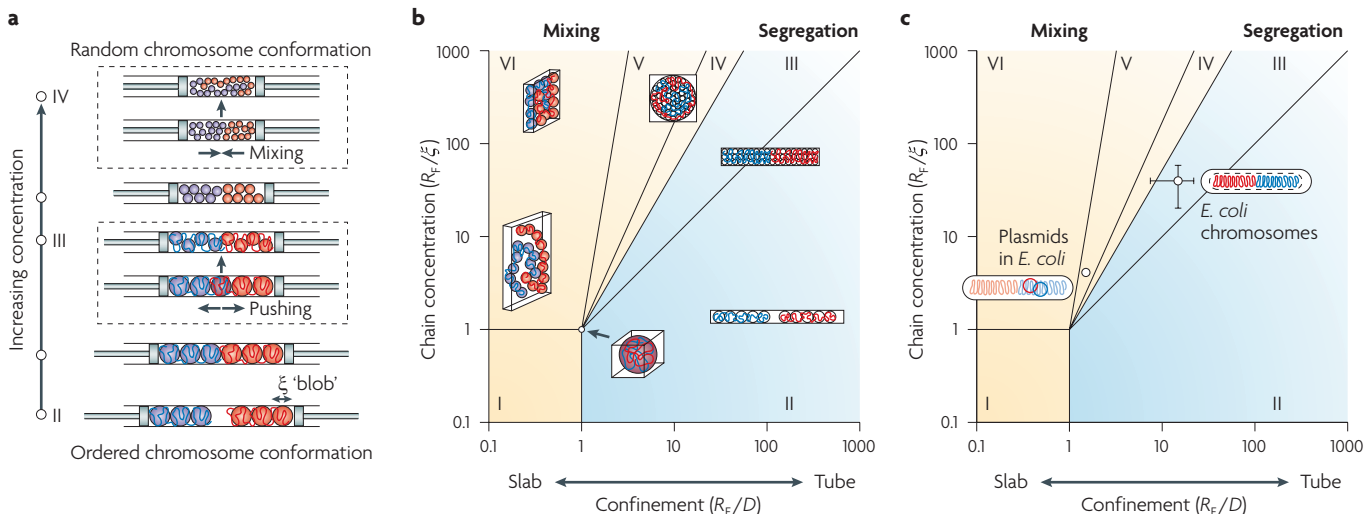


Figure 1 | Predicting chromosome segregation using physical parameters of the nucleoid. a | The piston analogy, illustrating the effect of the degree of confinement on the organization of two chains. Two long chains are confined in a cylinder of fixed width that is capped by two pistons. As the volume of the cylinder is decreased by the pistons, chains go through two simultaneous transitions: a change in the principal ordering of each chain from linear to random, and from segregation to mixing of the two chains. **b |** A phase diagram explaining how two long chains will segregate or mix depending on the degree of

confinement and the concentration of the chains in a box. This phase diagram can be used to predict the entropy-driven segregability of other organisms (see main text and Supplementary information S4 (box) for details). **c |** *Escherichia coli* chromosomes are in the segregation regime, whereas plasmids are in the mixing regime because they are too small. ξ , size of the structural unit (also called the correlation length); D , width of the nucleoid inside the cell; R_f , Flory radius of gyration of the isolated nucleoid released from the lysed cell.

in our phase diagram, as it would add a third dimension to the diagram for which quantitative results are currently unknown. Nevertheless, polymer physics makes the general prediction that an increased topological complexity of polymers (and membranes), such as branching, will only increase their tendency for segregation^{15,16}, and this will be especially strong in a confined space¹⁷. To see this intuitively, imagine two crumpled pieces of paper or nets with fine meshwork inside the cylinder in FIG. 1a. Unlike linear chains, they will never mix¹⁷. Another important factor at the cellular level is the symmetry break and invagination of the cell shape during division, which could help to resolve partially intermingled chromosomes. Indeed, real cells are never perfectly spherical. It has been shown numerically that pole-to-pole Min protein oscillations could be achieved along the long axis of a nearly round cell, in which the equatorial radii differ by as little as 5%¹⁸. This might explain the observed division of round cells at alternating perpendicular planes¹⁹.

Relationship with protein-based models

The phase diagram provides a quantitative framework for understanding the relationship between the physical state of the chromosome and its confinement and segregation, but under our reductionist

approach lie biological mechanisms orchestrated by proteins. Our hypothesis is that the role of these proteins is to change the physical state of the chromosome and, thus, create the right conditions for entropic segregation (TABLE 1). We describe below how our physical model is connected to other protein-based segregation models, making experimentally testable predictions where possible.

To this end, we first recapitulate the concentric-shell model for a replicating nucleoid¹⁵. This model was inspired by the observation that the fluorescently labelled *E. coli* nucleoid occupies a much smaller volume than the cell (BOX 1). In other words, the density of the chromosomal DNA should be much lower in the periphery of the *E. coli* nucleoid than at its core. The main prediction of the concentric-shell model is that newly synthesized DNA will be extruded to and will move in the periphery (the ‘outer shell’) of the nucleoid, in particular during the early stages of DNA replication (FIG. 2b). There are several advantages of this model. First, polymer repulsion is much stronger in the thin slab of the outer shell than in a space without confinement (see Supplementary information S4 (box)), so the replicating chromosome arms tend not to mix in the first place. Second, the replicating DNA can move much faster in the outer shell than inside the nucleoid

bulk (BOX 2). Third, moving in the outer shell allows the principal organization of the unreplicated nucleoid to be preserved and also facilitates the sequential deposition of newly synthesized DNA in the order of replication.

Our concentric-shell model can be tested experimentally. Berlitzky *et al.*²⁰ have developed a method for labelling replicating chromosomes in slow-growing *B. subtilis* cells using fluorescent nucleotide derivatives. Although their results are only qualitative, the technique shows great potential for tracking DNA duplicated before and after a chosen time point using two colours. Future experiments using this method for the careful quantitative analysis of cells in balanced growth may allow newly replicated DNA strands to be tracked throughout the cell cycle.

Active transport of plasmids and ori sites in some organisms. Low-copy-number plasmids segregate²¹ and position themselves inside the cell (for example, plasmid R1 at the cell poles, and plasmids P1 and F at the quarter positions)²² through dedicated mechanisms. There is also increasing experimental evidence that chromosomal origin (*ori*) loci are localized at specific intracellular positions in *E. coli* (at mid-cell)²³, *C. crescentus* (at old cell poles)²⁴ and *V. cholerae*^{25,26}. Consistent with these findings, it has been suggested

that bacterial cytoskeletal proteins such as plasmid partition protein M (ParM) and ParA are the machinery for active transport of low-copy-number plasmids and *ori* loci, respectively. The system consisting of ParA, ParB and *parS* (the binding site for ParB) is widely conserved in many bacteria and contributes to *ori* segregation in *C. crescentus* and *oriII* segregation in *V. cholerae*.

However, although ParA plays an important part in chromosome segregation, its role is likely to be limited, for the following reasons. In *C. crescentus*, ParA is not required once *ori* loci are separated at the beginning of the cell cycle²⁷. The absence of ParA alone has little effect on chromosome segregation in *B. subtilis*⁴, and there is no ParA homologue in *E. coli*. Also, as we discuss below, eukaryotic sister chromatids demix and move ~0.5 μm apart before their separation by spindles, without any active pushing or pulling of the replicated DNA²⁸. A potential problem with active transport of chromosomal *ori* loci for organisms that undergo multifork replication is that simple transport of multiple copies of *ori* may be harmful to the cell unless it also solves the ‘hierarchy dilemma’ of positioning an *ori* depending on its identity. An obvious experimental test of this idea would be to insert an active plasmid segregation system, such as ParM or the ParAB–*parS* system, into the *E. coli* chromosome. We predict that chromosome segregation during multifork replication in such an organism will be defective. We propose that organisms encoding ParA have adopted this protein from plasmids for a more efficient segregation of the *ori* domain, which is comparable in size to plasmids, rather than for segregation of the bulk chromosomes.

C. crescentus is smaller than *E. coli* and has a smaller cytoplasmic space surrounding its nucleoid, so the outer concentric shell of this species may not be large enough for fast diffusion of newly replicated DNA. In this case, ParA might be needed to ensure rapid segregation of the duplicated *ori* loci in the early stage of the replication cycle, when newly synthesized DNA would otherwise be kinetically trapped in the cell (see Supplementary information S4 (box)). The advantage of having an outer shell leads us to predict that, even in *C. crescentus*, duplicated *ori* loci will move in the periphery of the nucleoid. Finally, as the cell grows and replication continues, reducing the volume of the dense, unreplicated-DNA core, an outer shell is not needed for entropy-driven segregation¹⁵. The *C. crescentus* cell cycle is longer than those of *E. coli* and *B. subtilis*, which will further help segregation by entropy.

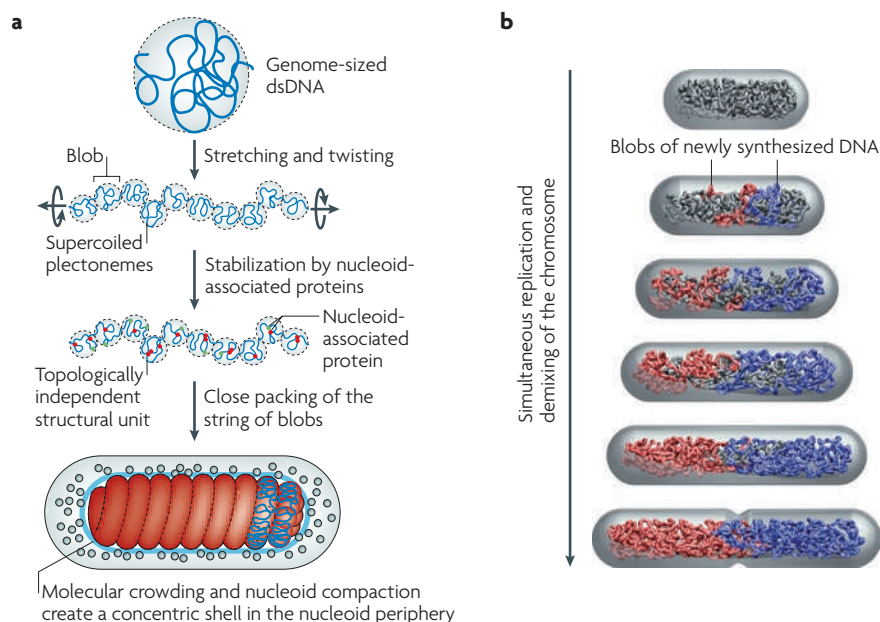


Figure 2 | Physical model of a bacterial chromosome and its segregation. **a** | A reductionist model of the *Escherichia coli* chromosome. First, we stretch a bacterial-genome-sized naked double-stranded DNA (dsDNA). This breaks the DNA into a series of blobs, the total volume of which gradually decreases as pulling continues. In parallel, we also twist the DNA to match the supercoil density of a bacterial chromosome. As a result, the DNA blobs will consist of supercoiled plectonemes (a shape of the DNA in which the two strands are intertwined). We stop the simultaneous pulling and twisting processes when the total volume of the blobs equals the target volume of the nucleoid inside the cell. Next, we ‘sprinkle’ the chromosome with nucleoid-associated proteins. These stabilize the supercoiled DNA blobs as topologically independent structural units of the chromosome. Finally, we connect the two ends of the chromosome to make it circular, and then pack it tightly in the cell. For the simpler case of chains without supercoiling, the phase diagram in FIG. 1 provides a model for the close-packed organization and segregability of the chains inside the cell. In general, supercoiling will only increase the tendency for chromosome demixing because of the branched structure that it induces. **b** | The concentric shell model predicts extrusion of the newly synthesized DNA (blue and red) to the periphery of the nucleoid¹⁵. The newly replicated DNA is extruded to the periphery of the unreplicated nucleoid (grey) and forms a string of DNA blobs in the order of replication, promoted by SMC (structural maintenance of chromosomes) proteins and other nucleoid-associated proteins. In our model, the two strings of blobs repel each other and drift apart owing to the excluded-volume interaction and conformational entropy.

Several proteins are involved in active transport of DNA inside a bacterium. Examples include SpoIIIIE, which moves DNA into the forespore during sporulation of *B. subtilis*, and FtsK, which resolves dimers and carries out other ‘rescue’ tasks in *E. coli*²⁹. However, it is important to realize that these proteins translocate DNA at the last step of segregation by taking advantage of the directionality that is provided by the septum, which is an entirely different process from segregation of replicating chromosomes.

Segregation models based on replication, transcription, translation and tethering. In addition to the active DNA transport models, both the force of DNA ejection by DNA polymerase and the tethering of DNA polymerase have been proposed to

move DNA in the cell. The finding of a fixed replication factory in *B. subtilis* led to the proposal of an ‘extrusion–capture’ model³⁰, which assumed that the energy released during replication could contribute to chromosome partitioning. Recent work, however, has shown that replication forks and their associated replisomes are both independent and highly dynamic in the cell, making their role in segregation unlikely^{31–33}. It was suggested that the negative effects of streptolydigin on polymerases in chromosome segregation³⁴. In addition, it has been proposed that translocation (the insertion of polypeptides into membranes during translation), instead of polymerases themselves, could segregate the replicating chromosomes³⁵. Definitive experimental support for these proposals is

Table 1 | Comparisons of the proposed segregation factors

Segregation factors	Remarks	Our interpretation
Chromosome tethering to the membrane and growth ⁵⁵	• The replicated ori moves much faster than the elongation rate of the cell ²⁴	• This may play a part in maintaining the DNA in the concentric shell
MreB ⁵⁶ (an actin homologue)	• <i>Escherichia coli</i> and filamentous cyanobacteria are viable without MreB ^{57,58} • For <i>Caulobacter crescentus</i> , the role of MreB is conditional ²⁷ • A recent study shows the functional interaction between MreB and Topo IV ⁴⁰	• This could contribute to efficient segregation by maintaining a high aspect ratio of the cell
ParM ⁶ (an actin homologue)	• This has been described as a factor involved in plasmid segregation	• ParM is not conserved in all bacteria and probably only functions for plasmids
ParA ²⁷	• This has been described as a factor involved in plasmid segregation • For chromosomes, it has a proposed role in ori movement in the initial stage of the cell cycle in <i>C. crescentus</i> and <i>Vibrio cholerae</i> ^{25,27} • There is no evidence for a role in bulk chromosome segregation	• This may help to extrude the newly synthesized DNA to the periphery of the nucleoid • It is particularly helpful for the initial separation of the duplicated ori, when there is not enough DNA-scarce space in the periphery of the nucleoid in some organisms (for example, <i>C. crescentus</i>)
migS and the bacterial 'centromere' (REF. 59)	• The mutant has a minor phenotype ⁵⁹	• It is unlikely that the putative bacterial 'centromere' plays a notable role in bulk chromosome segregation
MukB ⁶⁰ and SMC proteins	• Cells are usually conditionally viable without them ^{4,23}	• These proteins increase the correlation length of the chromosome to promote efficient segregation • They have interchangeable roles with other factors that increase the repulsive interactions between DNA (for example, an increased level of negative supercoiling)
Extrusion–capture ³⁰	• Replication forks are independent in slow-growing <i>E. coli</i> cells ^{31,32}	• This may help to extrude the newly synthesized DNA to the periphery of the nucleoid
RNA polymerase ³⁴	• Its role can be tested by the run-off DNA synthesis experiment (that is, by blocking protein synthesis)	• This may help to extrude the newly synthesized DNA to the periphery of the nucleoid
Coupling of transcription and translation, and membrane translocation ³⁵	• Its role can be tested by the run-off DNA synthesis experiment (that is, by blocking protein synthesis)	• This may help to extrude the newly synthesized DNA to the periphery of the nucleoid
Mechanical pushing (can be induced by cohesion) ^{47,48}	• Although they differ in their biological details, this model has the same view as the entropy model: that the intrinsic physical and mechanical properties of the chromosome are important for its biological function	• This can be understood in terms of excluded-volume interaction and conformational entropy
Excluded-volume interactions, chain-connectivity and conformational entropy ¹⁵	• The phase diagram presented in FIG. 1 explains the demixing of individual bulk chromosomes but does not consider the segregation of multiple chromosomes • Current work should be extended to incorporate the effect of chromosome topology (for example, the branched structure of supercoiled plectonemes)	• NA

NA, not applicable; ori, origin; Par, plasmid partition protein; SMC, structural maintenance of chromosomes.

lacking and, in fact, the translocation model is inconsistent with the speed of separation of chromosomal loci, especially those near the *ori*. But even if these factors do play a part in segregation, they would not be mutually exclusive with the entropy model or with other mechanical models. For example, they could support the concentric-shell model, as large macromolecular complexes such as replisomes would be extruded to the outer shell of the nucleoid. The outer shell is also a site of active transcription and is juxtaposed to the cell membrane, facilitating the translocation process. Translocation might effectively pull the newly synthesized DNA into the outer shell of the nucleoid and

then anchor it there. From our view, a more important consequence of translocation might be that completely duplicated nucleoids would be physically separated as a result of nucleoid association with the slowly growing cytoplasmic membrane.

Physical state of the chromosome. Perhaps the most important feature of our physical model of chromosome segregation is its robustness. In other words, the model does not depend on the microscopic organization of the chromosome in the structural unit (the blob) or on details of how individual proteins interact with the DNA. What is important is the size of the structural unit

— that is, the effective correlation length (ξ). As discussed above (and illustrated in FIG. 1a,b), a larger blob size always results in better segregation and more ordered chain conformations. (see also REF. 36 for computer simulation results; the authors observed segregation failure only when the structural units are small). In view of this, the most obvious candidates for increasing the size of the structural unit are the chromosome condensation proteins (the SMC proteins^{4,5} and *MukB*²³) and the small DNA-binding proteins (such as HU, H-NS and integration host factor (IHF))⁹. DNA gyrases are also important because they cause branched supercoils, promoting repulsive interactions

between the chromosomes. In this case, the torsional energy generated by DNA gyrase activity is used for topological repulsion between the supercoiled chromosomes.

Our theoretical argument is supported by studies showing that the disruption of chromosome segregation caused by a deficit in MukB is substantially (but not completely) alleviated by alterations in DNA gyrase activity, leading to increased levels of negative supercoiling^{14,36–38}. Although these data might suggest that redundant mechanisms help to drive chromosome segregation, we propose that neither class of protein forms the dedicated segregation machinery. Instead, we posit that their role is to maintain the chromosome in a specific physical condition that allows for entropy-driven segregation.

Cell growth, shape and division. As we illustrate in FIG. 1, a larger cell size means a lower concentration of chromosomal DNA (assuming that the amount of DNA remains constant), and this results in a larger ξ and better physical conditions for segregation. Similarly, a longer cell means a stronger tendency for segregation. Consequently, proteins that regulate cell growth and division are also important for ensuring that the cell reaches the appropriate size for proper segregation. Recent studies showed that *B. subtilis* possesses a metabolic sensor that couples nutrition availability to division, ensuring that cells reach the appropriate mass and complete chromosome segregation before cytokinesis³⁹. Similarly, other proteins can help segregation indirectly through secondary effects. The cytoskeletal protein MreB, for example, helps the cell maintain a higher aspect ratio and possibly also promotes chromosome segregation in the final stages by regulating the activity of topoisomerase IV at mid-cell⁴⁰.

Symmetry of the chromosome arms. Recently, an interesting observation on the distribution of chromosome arms (replicohores) in *E. coli* was reported^{41,42}. Under conditions in which cell cycles do not overlap, the *E. coli* nucleoid is linearly ordered, each replicohore occupies one half of the cell volume and the chromosome arms segregate progressively in the order of replication⁴³. Measuring the cell-to-cell positional variations of chromosomal markers allowed the effective spring constant of the *in vivo* nucleoid to be measured⁴⁴. A more recent striking observation comes from an elegant study showing that leading and lagging strands go to different cellular destinations⁴⁵. These findings are consistent with our model, in principle. For example, we

think that the physical constraints exerted by the core of the nucleoid itself and the required movement in the outer concentric shell, together with demixing and the physical difference between leading and lagging strands, may result in the symmetry seen. Indeed, data show that the organization of the *E. coli* chromosome throughout the cell cycle is determined by its evolving intrinsic mechanical and physical properties, which alter under the combined effects of repulsion and radial confinement (A. Bourniquel, M. Prentiss and N. Kleckner, personal communication). However, it will be necessary to add organism-specific instructions to our general physical model to explain the detailed differences between organisms such as *C. crescentus*^{24,27} (in which the *ori* is at the pole and is possibly tethered) and *E. coli* (in which leading and lagging strands display differential motions in the outer shell)^{45,46}. Future studies need to address the biological importance of these findings as well as their applicability to fast-growing cells and round cells.

Concluding remarks

One of the most striking events during the eukaryotic cell cycle is the separation of compact sister chromatids, aligned across the central plane of the cell, by the mitotic spindles. This hallmark of mitosis has inspired numerous proposals aimed at connecting bacterial chromosome segregation with the mitotic process. However, analogies between the two domains of life, such as the presence of a bacterial ‘centromere’ or ‘mitotic machinery’, have contributed little to our understanding of bulk chromosome segregation in bacteria. In this Opinion article, we argue that the active segregation mechanisms are present for the segregation of low-copy-number plasmids and can also be used for the positioning of *ori* sites in some bacterial organisms, perhaps as a product of evolution, but are not used for the chromosome bulk.

As previously noted by several researchers^{4,28,47–49}, it is important to realize that eukaryotic chromosomes also go through a period of intermingling during replication and that they demix without the help of mitotic spindles or any of the analogous protein-based mechanisms that have been proposed for bacterial chromosome segregation. It is known that topoisomerase II, condensins and histones are needed to build mitotic chromosomes and segregate sister DNA strands in eukaryotes, but the driving force behind the formation of sister chromatids with largely separated DNA has been unclear. The key question here is: what guiding force causes topoisomerase to

remove catenations rather than add them? We propose that entropic demixing provides the guiding force and directionality for sister strand separation during mitotic chromosome assembly, just as it does for bacterial chromosome segregation (BOX 2).

Further, the presence of multiple chromosomes poses an additional challenge for chromosome segregation in eukaryotic cells, because each daughter cell must receive not only the correct number but also the correct set of chromosomes. From our point of view, this strongly supports the argument that mitosis requires a more sophisticated, active segregation machinery and checkpoint, whereas entropy alone might be sufficient for chromosome segregation in most bacteria.

Finally, we would like to remind the reader that segregation by entropic forces, whether it is for bacterial chromosomes or eukaryotic sister chromatids, represents a robust mechanism. Although the diversity of life is the consequence of evolution, the robust nature of the physical principles in general, such as the example in chromosome segregation described here, may provide deeper insight into the basic processes shared by all life forms.

Suckjoon Jun is at the FAS Center for Systems Biology, Harvard University, Cambridge, Massachusetts 02138, USA.

Andrew Wright is at the Department of Molecular Biology and Microbiology, Tufts University School of Medicine, 136 Harrison Avenue, Boston, Massachusetts 02111, USA.

e-mails: sjun@cgr.harvard.edu; andrew.wright@tufts.edu

doi:10.1038/nrmicro2391

1. Kornberg, A. & Baker, T. A. *DNA Replication* 2nd edn (Freeman & Company, New York, 1992).
2. Murray, A. & Hunt, T. (eds) *The Cell Cycle: an Introduction*. (Oxford Univ. Press, New York, 1993).
3. Wang, J. C. DNA topoisomerases. *Annu. Rev. Biochem.* **65**, 635–692 (1996).
4. Sullivan, N. L., Marquis, K. A. & Rudner, D. Z. Recruitment of SMC to the origin by ParB-parS organizes the origin and promotes efficient chromosome segregation. *Cell* **137**, 697–707 (2009).
5. Gruber, S. & Errington, J. Recruitment of condensin to replication origin regions by ParB/SpoOJ promotes chromosome segregation in *B. subtilis*. *Cell* **137**, 685–696 (2009).
6. Salje, J., Zuber, B. & Löwe, J. Electron cryomicroscopy of *E. coli* reveals ParM filament bundles involved in plasmid segregation. *Science* **323**, 509–512 (2009).
7. deGennes, P.-G. *Scaling Concepts in Polymer Physics* (Cornell Univ. Press, Ithaca, New York, 1979).
8. Bloom, K. & Joglekar, A. Towards building a chromosome segregation machine. *Nature* **463**, 446–456 (2010).
9. Stavans, J. & Oppenheim, A. DNA-protein interactions and bacterial chromosome architecture. *Phys. Biol.* **3**, R1–R10 (2006).
10. Woldringh, C. L. & Odijk, T. in *Organization of the Prokaryotic Genome* (ed. Charlebois, R. L.) 171–187 (American Society for Microbiology, Washington DC, 1999).
11. Romantsov, T., Fishov, I. & Krichevsky, O. Internal structure and dynamics of isolated *Escherichia coli* nucleoids assessed by fluorescence correlation spectroscopy. *Biophys. J.* **92**, 2875–2884 (2007).

12. Derman, A. I., Lim-Fong, G. & Pogliano, J. Intracellular mobility of plasmid DNA is limited by the ParA family of partitioning systems. *Mol. Microbiol.* **67**, 935–946 (2008).
13. Jun, S., Arnold, A. & Ha, B.-Y. Confined space and effective interactions of multiple self-avoiding chains. *Phys. Rev. Lett.* **98**, 128303 (2007).
14. Sawitzke, J. A. & Austin, S. Suppression of chromosome segregation defects of *Escherichia coli* muk mutants by mutations in topoisomerase I. *Proc. Natl Acad. Sci. USA* **97**, 1671–1676 (2000).
15. Jun, S. & Mulder, B. Entropy-driven spatial organization of highly confined polymers: lessons for the bacterial chromosome. *Proc. Natl Acad. Sci. USA* **103**, 12388–12393 (2006).
16. Trun, N. J. & Marko, J. F. Architecture of a bacterial chromosome. *ASM News* **64**, 276–283 (1998).
17. Vilgis, T. A. Polymer theory: path integrals and scaling. *Phys. Rep.* **336**, 167–254 (2000).
18. Huang, J. C. & Wingreen, N. Min-protein oscillations in round bacteria. *Phys. Biol.* **1**, 229–235 (2004).
19. Corbin, B. D., Yu, X.-C. & Margolin, W. Exploring intracellular space: function of the Min system in round-shaped *Escherichia coli*. *EMBO J.* **21**, 1998–2008 (2002).
20. Berlitzky, I. A., Rovinsky, A. & Ben-Yehuda, S. Spatial organization of a replicating bacterial chromosome. *Proc. Natl Acad. Sci. USA* **105**, 14136–14140 (2008).
21. Nordstrom, K. & Austin, S. J. Mechanisms that contribute to the stable segregation of plasmids. *Annu. Rev. Genet.* **23**, 37–69 (1989).
22. Gordon, G. S. *et al.* Chromosome and low copy plasmid segregation in *E. coli*: visual evidence for distinct mechanisms. *Cell* **90**, 1113–1121 (1997).
23. Danilova, O., Reyes-Lamothe, R., Pinsky, M., Sherratt, D. & Possoz, C. MukB colocalizes with the *oriC* region and is required for organization of the two *Escherichia coli* chromosome arms into separate cell halves. *Mol. Microbiol.* **65**, 1485–1492 (2007).
24. Viollier, P. H., Thanbichile, M., McGrath, P. T., West, L. & Meewan, M. Rapid and sequential movement of individual chromosomal loci to specific subcellular locations during bacterial DNA replication. *Proc. Natl Acad. Sci. USA* **101**, 9257–9262 (2004).
25. Fogel, M. A. & Waldor, M. K. A dynamic, mitotic-like mechanism for bacterial chromosome segregation. *Genes Dev.* **20**, 3269–3282 (2006).
26. Fiebig, A., Keren, K. & Theriot, J. A. Fine-scale time-lapse analysis of the biphasic, dynamic behaviour of the two *Vibrio cholerae* chromosomes. *Mol. Microbiol.* **60**, 1164–1178 (2006).
27. Toro, E., Hong, S.-H., McAdams, H. H. & Shapiro, L. *Caulobacter* requires a dedicated mechanism to initiate chromosome segregation. *Proc. Natl Acad. Sci. USA* **105**, 15435–15440 (2008).
28. Nasmyth, K. Segregating sister genomes: the molecular biology of chromosome separation. *Science* **297**, 559–565 (2002).
29. Barre, F.-X. FtsK and SpollIE: the tale of the conserved tails. *Mol. Microbiol.* **66**, 1051–1055 (2007).
30. Lemon, K. P. & Grossman, A. D. The extrusion capture model for chromosome partitioning in bacteria. *Genes Dev.* **15**, 2031–2041 (2001).
31. Migocki, M. D., Lewis, P. J., Wake, R. G. & Harry, E. J. The midcell replication factory in *Bacillus subtilis* is highly mobile: implications for coordinating chromosome replication with other cell cycle events. *Mol. Microbiol.* **54**, 452–463 (2004).
32. Bates, D. The bacterial replisome: back on track? *Mol. Microbiol.* **69**, 1341–1348 (2008).
33. Reyes-Lamothe, R., Possoz, C., Danilova, O. & Sherratt, D. J. Independent positioning and action of *Escherichia coli* replisomes in live cells. *Cell* **133**, 90–102 (2008).
34. Dworkin, J. & Losick, R. Does RNA polymerase help drive chromosome segregation in bacteria? *Proc. Natl Acad. Sci. USA* **99**, 14089–14094 (2002).
35. Woldringh, C. L. The role of co-transcriptional translation and protein translocation (translocation) in bacterial chromosome segregation. *Mol. Microbiol.* **45**, 17–29 (2002).
36. Fan, J., Tuncay, K. & Ortoleva, P. J. Chromosome segregation in *Escherichia coli* division: a free energy-driven string model. *Comput. Biol. Chem.* **31**, 257–264 (2007).
37. Holmes, V. F. & Cozzarelli, N. R. Closing the ring: links between SMC proteins and chromosome partitioning, condensation, and supercoiling. *Proc. Natl Acad. Sci. USA* **97**, 1322–1324 (2000).
38. Dasgupta, S., Maisnier-Patin, S. & Nordstrom, K. New genes with old *modus operandi*: the connection between supercoiling and partitioning of DNA in *Escherichia coli*. *EMBO Rep.* **1**, 323–327 (2000).
39. Weart, R. B. *et al.* A metabolic sensor governing cell size in bacteria. *Cell* **130**, 335–347 (2007).
40. Madabushishi, R. & Marrias, K. J. Active homolog MreB affects chromosome segregation by regulating topoisomerase IV in *Escherichia coli*. *Mol. Cell* **33**, 171–180 (2009).
41. Wang, X., Liu, X., Possoz, C. & Sherratt, D. J. The two *Escherichia coli* chromosome arms locate to separate cell halves. *Genes Dev.* **20**, 1727–1731 (2006).
42. Nielsen, H. J., Ottensen, J. R., Youngren, B., Austin, S. J. & Hansen, F. G. The *Escherichia coli* chromosome is organized with the left and right chromosome arms in separate cell halves. *Mol. Microbiol.* **62**, 331–338 (2006).
43. Nielsen, H. J., Li, Y., Youngren, B., Hansen, F. G. & Austin, S. J. Progressive segregation of the *Escherichia coli* chromosome. *Mol. Microbiol.* **61**, 383–393 (2006).
44. Wiggins, P. A., Cheveralls, K., Martin, J. S., Lintner, R. & Kondev, J. Strong intranucleoid interactions organize the *Escherichia coli* chromosome into a nucleoid filament. *Proc. Natl Acad. Sci. USA* **107**, 4991–4995 (2010).
45. White, M. A., Eykelenboom, J. K., Lopez-Vernaza, M. A., Wilson, E. & Leach, D. R. F. Non-random segregation of sister chromosomes in *Escherichia coli*. *Nature* **455**, 1248–1250 (2008).
46. Reyes-Lamothe, R., Wang, X. & Sherratt, D. *Escherichia coli* and its chromosome. *Trends Microbiol.* **16**, 238–245 (2008).
47. Kleckner, N. *et al.* A mechanical basis for chromosome function. *Proc. Natl Acad. Sci. USA* **101**, 12592–12597 (2004).
48. Bates, D. & Kleckner, N. Chromosome and replisome dynamics in *E. coli*: loss of sister cohesion triggers global chromosome movement and mediates chromosome segregation. *Cell* **121**, 899–911 (2005).
49. Woldringh, C. L. & van Driel, R. in *Organization of the Prokaryotic Genome* Ch. 5 (ed. Charlebois, R. L.) 77–90 (American Society for Microbiology, Washington DC, 1999).
50. Schrödinger, E. *What is life?* (Cambridge Univ. Press, Cambridge, UK, 1944).
51. Flory, P. *Principles of Polymer Chemistry* (Cornell Univ. Press, Ithaca, New York, 1953).
52. Grosberg, A. Y., Khalatur, P. G. & Khokhlova, A. R. Polymeric coils with excluded volume in dilute solution: the invalidity of the model of impenetrable spheres and the influence of excluded volume on the rates of diffusion-controlled intermacromolecular reactions. *Makromol. Chem. Rapid Commun.* **3**, 709–713 (1982).
53. Pincus, P. Excluded volume effects and stretched polymer chains. *Macromolecules* **9**, 386–388 (1976).
54. Liu, Z., Zechedrich, E. L. & Chan, H. S. Inferring global topology from local juxtaposition geometry: interlinking polymer rings and ramifications for topoisomerase action. *Biophys. J.* **90**, 2344–2355 (2006).
55. Jacob, F., Brenner, S. & Cuzin, F. On the regulation of DNA replication in bacteria. *Cold Spring Harb. Symp. Quant. Biol.* **28**, 329–348 (1963).
56. Kruse, T. & Gerdes, K. Bacterial DNA segregation by the actin-like MreB protein. *Trends. Cell Biol.* **15**, 343–345 (2005).
57. Hu, B., Yang, G., Zhao, W., Zhang, Y. & Zhao, J. MreB is important for cell shape but not for chromosome segregation of the filamentous cyanobacterium *Anabaena* sp. PCC 7120. *Mol. Microbiol.* **63**, 1640–1652 (2007).
58. Karczmarek, A. *et al.* DNA and origin region segregation are not affected by the transition from rod to sphere after inhibition of *Escherichia coli* MreB by A22. *Mol. Microbiol.* **65**, 51–63 (2007).
59. Yamaichi, Y. & Niki, H. *migS*, a *cis*-acting site that affects bipolar positioning of *oriC* on the *Escherichia coli* chromosome. *EMBO J.* **23**, 221–233 (2004).
60. Niki, H., Jaffe, A., Imamura, R., Ogura, T. & Hiraga, S. The new gene *mukB* codes for a 177 kD protein with coiled-coil domains involved in chromosome partitioning of *E. coli*. *EMBO J.* **10**, 183–193 (1991).

Acknowledgements

We are deeply grateful to T. Mitchison for his penetrating insight and numerous invaluable suggestions. We thank N. Kleckner and C. Woldringh for critical reading of the manuscript. We also thank J.-Y. Bouet, A. Brouniquel, A. Danchin, E. Garner, B.-Y. Ha, R. Losick, K. Maeshima, B. Mulder, A. Murray, P. Wiggins and many other colleagues for helpful discussions over the years. This work was supported by Harvard University, USA, and the US National Institutes of Health (grant P50 GM068763 to S.J.).

Competing interests statement

The authors declare no competing financial interests.

DATABASES

Entrez Genome Project: <http://www.ncbi.nlm.nih.gov/genomeprj>
Bacillus subtilis | *Caulobacter crescentus* | *Escherichia coli* | *Vibrio cholerae*
UniProtKB: <http://www.uniprot.org>
FtsK | *H-NS* | *MreB* | *MukB* | *ParA* | *ParB* | *ParM* | *SpollIE*

FURTHER INFORMATION

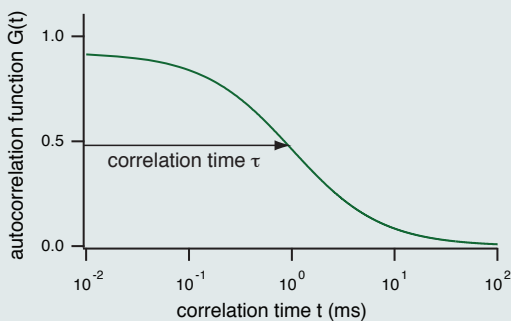
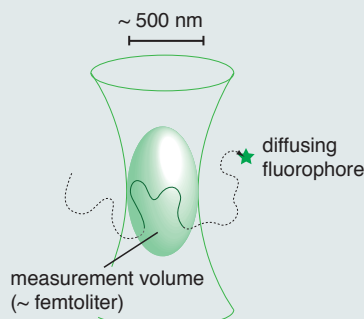
Suckjoon Jun's homepage: <http://www.sysbio.harvard.edu/csb/jun/>
Andrew Wright's homepage: <http://sackler.tufts.edu/Academics/Degree-Programs/PhD-Programs/Faculty-Research-Pages/Andrew-Wright.aspx>

SUPPLEMENTARY INFORMATION

See online article: [S1](#) (movie) | [S2](#) (movie) | [S3](#) (box) | [S4](#) (box)

ALL LINKS ARE ACTIVE IN THE ONLINE PDF

S3 | Measuring the size of the structural unit of chromosome with fluorescence correlation spectroscopy (FCS)

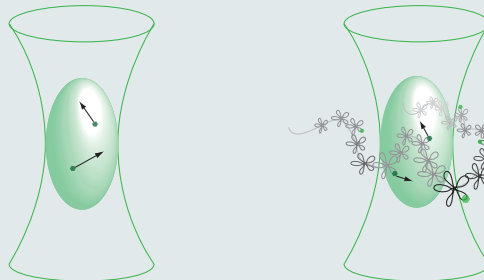


FCS is a simple but powerful tool to study dynamics of fluorescently labelled biomolecules such as proteins and DNA. As fluorophores diffuse through the measurement volume of the focused laser beam, they emit photons (left). From measurements of the corresponding fluctuations in fluorescence intensity over time, an autocorrelation curve can be calculated (right). Each autocorrelation curve contains information about the average number of particles, N , diffusing through the volume [$G(0) = 1/N$], as well as the characteristic correlation time τ for the diffusion process. The correlation time τ_D is related to the diffusion constant D and the width of the measurement volume w by $D = w^2/4\tau_D$.

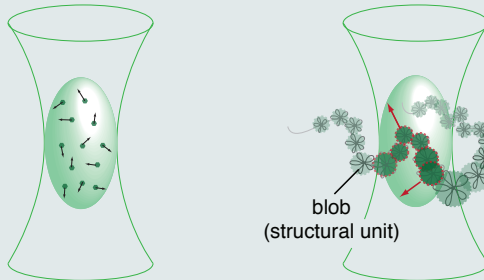
FCS can also be used not only to probe the characteristic timescale of the motion of a chromosome labelled with fluorophores, but also to measure the size of its correlation length. Over the timescale of measurement the chromosome as a whole is virtually immobile, thus the fluctuations in fluorescence are caused solely by the internal dynamics of the chromosome, for example, by the motion and conformational changes of its structural units. At low fluorophore densities, the distances between bound fluorophores are large, their positions are uncorrelated, and their motions are independent of each other (top right). At such densities, the apparent number of independent fluorescence sources is $N=1/G(0)$, just like the case of freely diffusing fluorophores (top left).

As fluorophore density increases, fluorophore positions and motions become increasingly correlated since numerous dye molecules label each structural element of the chromosome, in strong contrast to freely diffusing fluorophores (bottom left). At the limit of high fluorophore densities, $1/G(0)$ becomes the number of structural units in the measurement volume, since each structural unit behaves as if it is an independent source of fluorescence. This elegant idea is the basis of mathematically more involved analysis by Krichevsky and co-workers, who estimated the size of the structural unit of the isolated *E. coli* nucleoid (about 90 nm) by iterating their FCS measurements at varying fluorophore densities¹.

freely diffusing fluorophores at low concentrations independent motions of the fluorophores bound to the chromosome at low densities



freely diffusing fluorophores at high concentrations correlated fluorophore motions inside the blob (structural unit) of the chromosome at high fluorophore densities



1. Romantsov, T., Fishov, I. & Krichevsky, O. Internal structure and dynamics of isolated *Escherichia coli* nucleoids assessed by fluorescence correlation spectroscopy. *Biophys. J.* **92**, 2875–2884 (2007).

**Supplementary Note for “Entropy as the driver of chromosome segregation”
by Jun and Wright.**

In this Supplementary Note, we describe the polymer physics related to the phase diagram in Fig. 1b and the relationship between the stretching and compression of a self-avoiding chain in Fig. 2a in the main text. We also explain in more details how we estimated where *E. coli* chromosomes and plasmids lie in the phase diagram. [Hereafter, “Fig.” refers to figures in the Supplementary Note unless specified otherwise.)]

CONTENTS

I. Polymer physics	2
A. More technical description of the phase diagram in Fig. 1 in the main text	2
B. Self-consistent mapping between the Pincus (stretched) and the close-packed chains.	5
C. Strong segregation in two-dimensional space	6
D. Chain topology and the phase diagram – branched polymers repel strongly	6
II. Application to bacterial chromosomes and plasmids.	7
A. Application to <i>E. coli</i> chromosomes.	7
B. Application to plasmid segregation.	8
References	8

I. POLYMER PHYSICS

In the main text, we used the piston analogy to illustrate how two linear polymers of the same size with excluded-volume interactions can mix and demix driven by conformational entropy depending on the confining geometry and its volume. Although we assumed that the confining box is characterized by two length scales: the width D and length L of the box, thus its cross-section is square of length D , it is straightforward to extend our results to a more general case where all three sides have different lengths.

Figure 1 in the next page quantitatively describes the phase diagram. The dimensionless quantity $x = R_F/D$ is the ratio of the size of the unperturbed chain (the Flory radius R_F) to the width of the cylinder; thus, the x -axis represents the degree of confinement the trapped chains feel from the side walls. The y -axis represents the concentration of the polymers in the box, since the chain correlation length (blob size), ξ_{bulk} , decreases monotonically as the monomer density of the chain increases.

A. More technical description of the phase diagram in Fig. 1 in the main text

Our phase diagram is divided into two regions, where chains segregate (blue) and mix (red) (Fig. 1), which can be further divided into six regimes. The boundary between segregation and mixing is given by the following simple geometric condition

$$k = \frac{L}{D} = \frac{D}{\xi_{\text{bulk}}}. \quad (1)$$

This is where the aspect ratio of the box becomes equal to the ratio of the width of the box to the size of the blobs. The rest of the phase diagram can be best understood as we move along the horizontal dotted line in Fig. 1. Since ξ_{bulk} depends only on the chain density, this line represents changing the aspect ratio of the confining box (k) from filamentous ($k > 1$) to slab-like ($k < 1$) through cubic/spherical ($k = 1$) shapes, keeping constant the volume of the box. Note that the longer the box the better segregation, and that the chains can readily mix and demix in a sphere ($k = 1$) (Jun *et al.*, 2007).

More detailed descriptions of the individual regimes are as follows, with relevant references so that the reader can reproduce the boundary conditions of the phase diagram. [See, also, Brochard and de Gennes (1979); Daoud and de Gennes (1977); Teraoka and Wang (2004)].

I. This is the “bulk” dilute regime, where the chains do not feel the confinement and the interchain distances are much larger than the size of the chain in confinement. When $D = L = R_F$, namely, a cube whose size equals the size of an unperturbed chain, the correlation length ξ_{bulk} also equals the size of the chain R_F , and the two chains can overlap at the free-energy cost of order $k_B T$ [Fig. 1(a)] (Grosberg *et al.*, 1982; Jun *et al.*, 2007).

II. Imagine dilute solution in a long cylindrical box, where there is a free space between the two chains [Fig. 1(b)]. The size of individual chains scales as $R_0 \sim (N/g)D \sim ND^{-2/3}$ (where g is the number of monomers per blob). In case of overlapping, the chains strongly repel one another and, thus, their segregation is much faster than reptation (typical timescale of $\tau \sim N^2$ vs. $\tau \sim N^3$, respectively) (Arnold and Jun, 2007; Jun and Mulder, 2006). The D dependence of the timescale of chain fluctuations is more subtle and significant finite-size effects have been reported (Arnold *et al.*, 2007; Jung *et al.*, 2009). Note that $\xi_{\text{bulk}} > D$ in this regime, whereas the blob size of the chain due to confinement is D . Thus, the monomer-monomer correlation length inside the box is $\xi_{\text{box}} = D < \xi_{\text{bulk}}$.

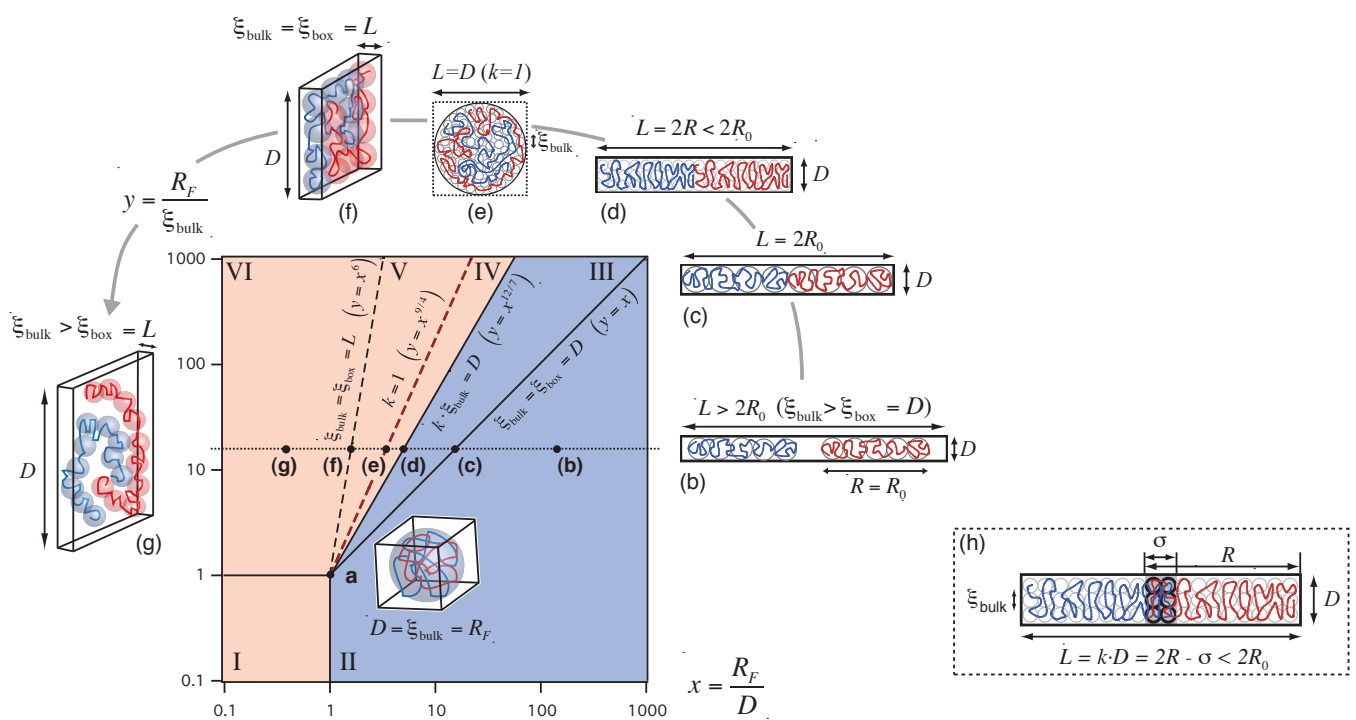


FIG. 1 Phase diagram of a 2-chain polymer solution confined in a closed geometry of dimensions $D \times D \times L$. The x -axis represents the shape of the geometry. The y -axis represents the concentration of the polymer solution. Regimes with a red background represent mixed states, while those with a blue background represent segregated states. The dotted horizontal line shows the effect of aspect ratio of confinement on two chains of constant length N . Shown along this line are a few representative chain conformations (b)-(g). For cubic confinement with side $D = R_F$ (a), two chains mix at the free-energy cost of order $k_B T$ (Grosberg *et al.*, 1982; Jun *et al.*, 2007). (h) Same as (d), but the two chains are in partial overlap of penetration depth σ . Due to compression, the correlation length ξ_{bulk} of the confined chains is smaller than the width of the rectangular box D (see the stacking blobs). [R_0 is the equilibrium end-to-end distance of an unperturbed chain in a long cylinder, and k the aspect ratio of the box.]

If we gradually reduce the aspect ratio of the box, keeping constant the volume of the box (thus, fixing ξ_{bulk}), the number of blobs of each chain decreases and eventually the two chains make contact at $L = 2R_0$, i.e., $\xi_{\text{bulk}} = \xi_{\text{box}} = D$ ($y = x$). This situation is depicted in Fig. 1(c), at which the chains enter the semi-dilute regime inside the elongated box.

III. If we continue the above process of reducing the aspect ratio of the box, the two chains are gradually compressed but do not mix as long as their principal conformations are linear [Fig. 1(d).] As we discussed in Sec. II.A, this is the most important regime for rod-shaped bacteria. To see the segregation of overlapping chains, let us employ the following Flory-type free energy of individual chains:

$$\beta\mathcal{F}_1(R) = \frac{1}{2} \left[\frac{R^2}{(N/g)D^2} + \frac{D(N/g)^2}{R} \right], \quad (2)$$

where $\beta = 1/k_B T$ (Jun *et al.*, 2008). Since it costs $\sim k_B T$ of free energy for two blobs to significantly overlap (Grosberg *et al.*, 1982; Jun *et al.*, 2007; Jun and Mulder, 2006), the total free energy of two partially overlapping chains in Fig. 1(h) can be written as

$$\begin{aligned} \beta\mathcal{F}_{\text{tot}} &= \left(2 + \frac{\sigma}{R}\right) \beta\mathcal{F}_1(R) \\ &= \frac{k}{2} \left(\frac{4}{L'} - \frac{1}{R'} \right) \left[R'^2 + \frac{1}{R'} \right], \end{aligned} \quad (3)$$

where $L' = L/R_0 \leq 2$, $R' = R/R_0 \leq 1$, $D' = D/R_0$. Since $\partial\beta\mathcal{F}_{\text{tot}}/\partial R' = 3k/2 > 0$ at $R' = L'/2$ (namely, when each chain occupies each cell half), Eq. 3 indeed predicts a free-energy barrier against mixing of two segregated chains. Moreover, one can show numerically that the free energy \mathcal{F}_{tot} is a monotonically increasing function of $R' \geq L'/2$ for

$$L' \gtrapprox 0.8.$$
¹

IV, *V*, *VI* (mixing regimes). As the aspect ratio approaches 1, the two chains lose their linear conformations and mix with each other. The reason for this transition is that the bulk correlation length ξ_{bulk} becomes much smaller than both D and L , and the chain conformation becomes a random walk of a string of blobs (blob size ξ_{bulk}). We described the physics of this regime in detail in [Jun et al. \(2007\)](#).

At the boundary between *III* and *IV*, transition occurs because individual chains are contracted and lose their linear ordering. The size of individual chain is that of the random-walk conformation, $R_{\parallel} \sim N^{1/2}\Phi^{-1/8}$ with the volume fraction of the monomer $\Phi \sim N/R_{\parallel}D$. Based on this, it is easy to show the boundary condition $y = x^{12/7}$ ([Lal et al., 1997](#)). Since the free energy in this regime is given by

$$\beta\mathcal{F}_{\text{IV}} \simeq \left(\frac{R_F^3}{D^2 L} \right)^{\frac{1}{3\nu-1}} \simeq \frac{D^2 L}{\xi_{\text{bulk}}^3} \quad (4)$$

([Cacciuto and Luijten, 2006](#); [Grosberg and Khokhlov, 1994](#); [Jun et al., 2007](#); [Sakaue and Raphaël, 2006](#)), the above boundary condition is translated to $D = k \cdot \xi_{\text{bulk}}$, symmetrical with another condition $L = k \cdot D$ we discussed previously. Similarly, it is straightforward to show that the boundary condition $k = 1$ between *IV* and *V* is identical to $y = x^{9/4}$ [Fig. 1(e)].

In regime *V*, the shape of the box resembles a thick slab. As the thickness of the slab reaches the size of the blob, i.e., $\xi_{\text{bulk}} = L = k \cdot D$ [Fig. 1(e)], the two chains enter the dilute regime in a thin, closed slab [Fig. 1(g)], which is the dual regime of *II*. Thus, the transition between *V* and *VI* occurs when the chains start to feel the size of the slab, i.e., at $D \sim R_{\parallel} \sim N^{1/2}\Phi^{-1/8}$, where the volume fraction is given by $\Phi \sim g/\xi_{\text{bulk}}^3$, with $g \sim \xi_{\text{bulk}}^{1/\nu}$. We thus obtain $y = x^6$ ($L = k \cdot D$).

Note that regime *V* should not be confused with two-dimensional confinement where polymer repulsion is much stronger (Sec. I.C). In the scaling regime in the three-dimensional slab, two chains can completely cross each other only at the cost of $\sim k_B T$ for single blob-blob overlap.

¹ Since the N^2/R dependence in Eq. 2 is an well-known overestimate of Flory-type approach for $R \ll R_0$, the $L' \approx 0.8$ is an upperbound. In other words, two chains should segregate in an even shorter box. For the same reason, we cannot use Eq. 3 to determine the condition for crossover to regime *IV*. For a more correct form of free energy for describing force-compression-stretching curves in cylindrical confinement, see [Jun et al. \(2008\)](#).

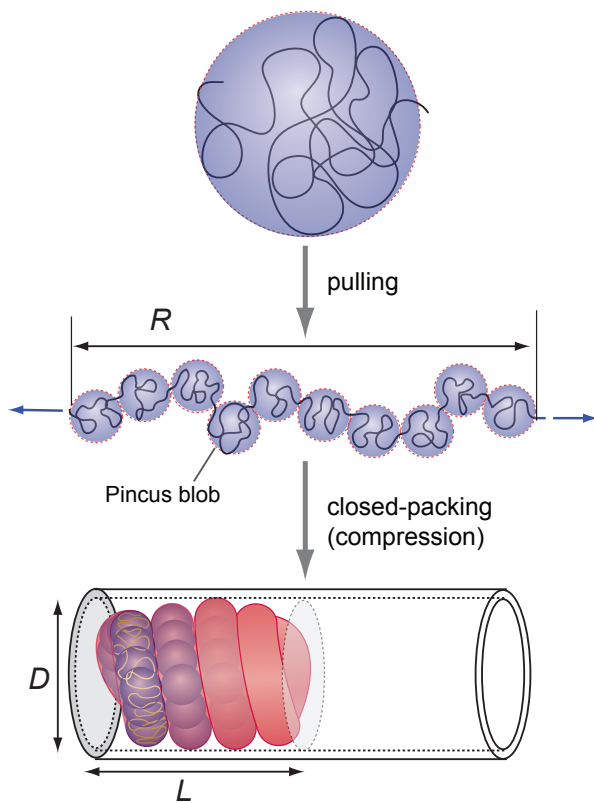


FIG. 2 In the scaling theory, stretching of a self-avoiding chain can be mapped onto compression of the chain via closed-packing into a confined space using the concept of blob. The compression free energy of the chain obtained this way is consistent with the results obtained by seemingly different methods Jun *et al.* (2007); Sakaue and Raphaël (2006).

B. Self-consistent mapping between the Pincus (stretched) and the close-packed chains.

In the Pincus picture of a stretched chain, the chain breaks up into a series of blobs of size ξ (Fig. 2). The free energy cost can be estimated by counting the number of blobs,

$$\beta\mathcal{F}_P \sim \frac{N}{g} \sim \frac{R}{\xi} \sim N \left(\frac{R}{N} \right)^{\frac{1}{1-\nu}}, \quad (5)$$

where $g \sim \xi^{1/\nu}$ is the number of monomers per blob and R the end-to-end distance of the chain.

Let us now imagine close-packing of the stretched chain consisting of blobs of size ξ into a cylinder of diameter D . Assuming this process does not cost any additional free energy, we can self-consistently obtain the confinement free energy accordingly as follows.

$$\beta\mathcal{F}_{\text{cyl}} \sim \frac{LD^2}{\xi^3} \sim N \left(\frac{R}{N} \right)^{\frac{1}{1-\nu}} \sim \left(\frac{LD^2}{N^{3\nu}} \right)^{\frac{1}{1-3\nu}}, \quad (6)$$

where L is the longitudinal size of the close-packed chain in the cylinder and we used Eq. 5. Equation 6 has the same scaling form of the free energy cost for confining a self-avoiding chain in a volume V ,

$$\beta\mathcal{F}_{\text{cyl}} \sim \left(\frac{V}{R_g^3} \right)^{\frac{1}{1-3\nu}} \quad (7)$$

(see Eq. 4), and we thus have a self-consistent picture for interpreting compressed chain based on the Pincus chain.

The essence of our analysis here is that the free energy for deformation can be mapped onto one another as long as the blob picture applies ($\sim k_B T/\text{blob}$).

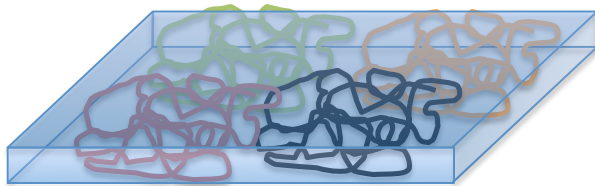


FIG. 3 Chains in two-dimensional space repel much more strongly than in three-dimension.

C. Strong segregation in two-dimensional space

So far, we have discussed polymer repulsion in three-dimensional confinement. In two-dimensional confinement like the outer-shell we hypothesized for *E. coli*, polymers will segregate more strongly as the concentration of the chain increases [Fig. 3]. This can be shown using the approach taken in Jun *et al.* (2007), which predicts that the free-energy cost of a chain overlapping crosses over from $\beta\mathcal{F} \sim n^{d\nu_d/(d\nu_d-1)}$ to $\sim n^{d/(d-2)}$, where $\nu_d = 3/(d+2)$ is the Flory exponent and d the spatial dimension. Thus, for $d = 3$, the free energy of chain mixing diverges at high chain concentration, i.e., chains will demix. Intuitively, segregation can be understood because, in 2D, a single chain can divide the space by “percolating” from wall-to-wall.

D. Chain topology and the phase diagram – branched polymers repel strongly

The bacterial chromosome poses an interesting question on the effect of chain topology. First, the literal topology of most bacterial chromosomes is not linear but circular. In bulk solutions without strong confinement, it is known that there is an additional topological repulsion between ring polymers due to the non-concatenation condition Cates and Deutsch (1986). However, in the presence of strong confinement, such “end effect” of the chain molecules will not change the overall picture for linear chains significantly, since the correlation length of the chain becomes much smaller than the size of the chain.

From segregation and polymer physics point of view, we believe that the most important feature of the bacterial chromosome is the presence of supercoiled plectonemes due to undertwisting of the DNA-helix. This makes the effective topology of the bacterial chromosome mimic branched, tree-like structures. Branched polymers have higher internal topological complexity, which makes the repulsive interactions much stronger than between linear or circular chains. For example, imagine a polymer chain forming a square-lattice-like meshwork. Such object is essentially a 2-dimensional membrane, which cannot interpenetrate one another, qualitatively different from overlapping between two linear chains. Branched chains stand between these two extreme cases (Fig. 4).

In principle, one may be able to add a third dimension to the phase diagram in Fig. 1 as illustrated in Fig. 4. Unfortunately, it poses a formidable mathematical challenges and our understanding is very limited except that we qualitatively expect the segregation regime will significantly extend to the mixing regime.

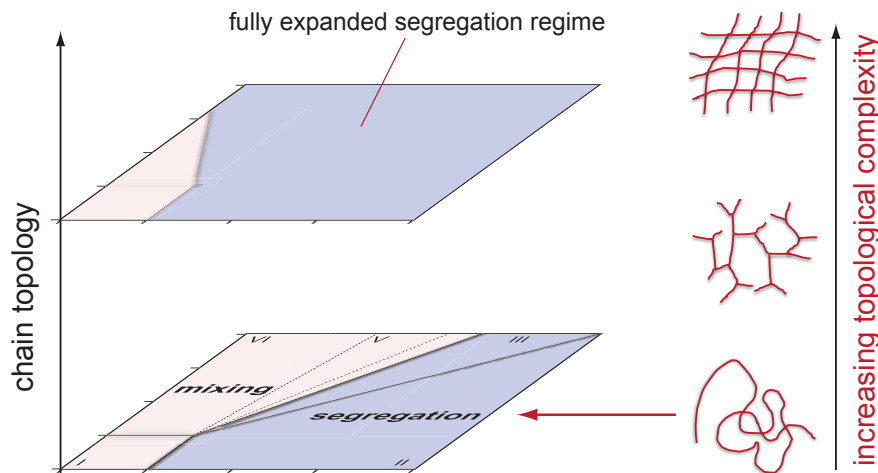


FIG. 4 Increasing topological complexity of the chain corresponds to stronger repulsion between them. This will add the third dimension to the phase diagram in Fig. 1, where we expect the segregation region will significantly expand to the mixing region as the topology changes from linear to branched.

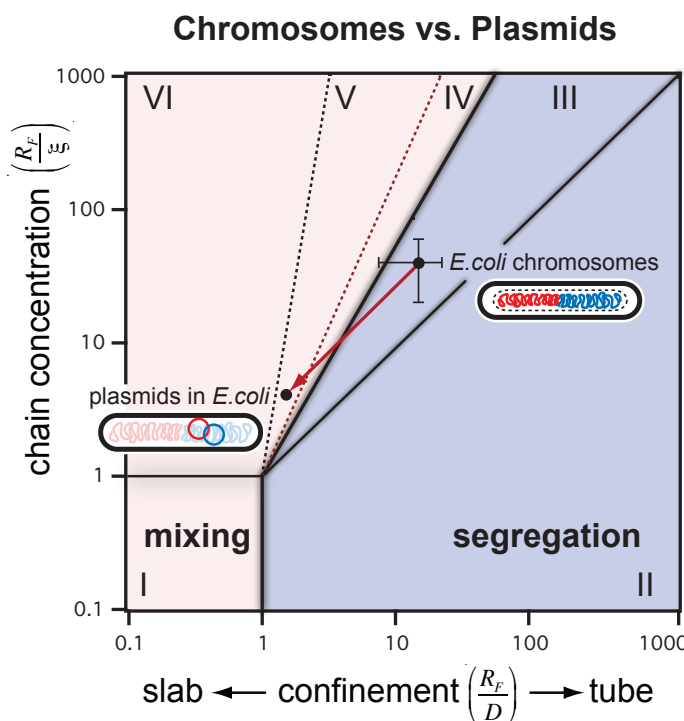


FIG. 5 Chromosome vs. plasmid. The two axes represent confinement ($x = R_F/D$) and chain concentration ($y = R_F/\xi$). For *E. coli* B/r (H266), we estimated $x = 13.6$ and $y = 37.5$ for the chromosome. Plasmids correspond to approximately one order of magnitude smaller values of x and y (see text).

II. APPLICATION TO BACTERIAL CHROMOSOMES AND PLASMIDS.

A. Application to *E. coli* chromosomes.

In the main text, we used our phase diagram to explain why duplicated bacterial chromosomes should stay segregated. We examined the model system *E. coli* B/r (H266), one of the most well-studied and well-documented bacterial strains (Woldringh and Odijk, 1999). Here we explain in more details.

When slowly growing at steady state with generation time of 150 minutes, the average length of *E. coli* B/r (H266) cell is 2.5 μm and the width 0.5 μm . However, the actual dimension in which chromosomes are confined inside a cell – the nucleoid – is smaller because of the well-known phenomena of nucleoid compaction (Woldringh and Odijk, 1999) as we discussed in the main text (see also Box 1). The measured diameter of the fluorescently-labeled *in vivo* nucleoid is about $D = 0.24 \mu\text{m}$ and $L_0 = 1.39 \mu\text{m}$ for new-born cells containing a single chromosome².

The correlation length ξ_{bulk} is a more difficult quantity to measure experimentally, because a number of factors contribute to chromosome organization in bacteria (e.g., molecular crowding, supercoiling and DNA-protein interactions) (Stavans and Oppenheim, 2006). Nevertheless, we can safely assume that the lower bound of ξ_{bulk} should be the persistence length of dsDNA, $\ell_p = 50\text{nm}$.³ Note that recent experimental studies have shown that there are as many as $\simeq 400$ topological domains in *E. coli* chromosome, corresponding $\simeq 10 \text{ kb}$ per domain (Deng *et al.*, 2005). If we assume that each domain occupies d^3 of a nucleoid volume, we obtain $d \simeq 53\text{nm}$, about the same as ℓ_p of bare DNA.

Very recently, Krichevsky and colleagues have measured ξ_{bulk} of nucleoid isolated from the same *E. coli* strain [B/r (H266)] using a more direct method of fluorescence correlation spectroscopy (FCS) (Romantsov *et al.*, 2007). We illustrated their method in Box 2 in the main text. The estimated size of the structural unit of the isolated nucleoid was about 50 kb, which corresponds to $d \simeq 87\text{nm}$ of the B/r *in vivo* chromosome [based on the nucleoid volume $\approx 0.06 \mu\text{m}^3$ (Woldringh and Odijk, 1999)]. Krichevsky and colleagues also calculated the physical size of the structural unit based on less direct measurement of the diffusion constant of isolated nucleoids. Their estimated value

² The population average is $\bar{L} = 1.8 \mu\text{m}$ (Woldringh and Odijk, 1999) with $L_0 \approx 0.7\bar{L}$ (Kubitschek, 1981), and we assumed a linear relationship between cell size and nucleoid length.

³ For supercoiled DNA, the persistence length of the plectoneme is estimated to be twice that of dsDNA Marko and Siggia (1995).

was $d = 70 \pm 20\text{nm}$, again, in good agreement with $d = 87\text{nm}$ above. Indeed, we have used these parameters including the average size of the isolated nucleoids $R_F = 3.3\mu\text{m}$ ([Romantsov et al., 2007](#)) (from the average spherical volume of natively supercoiled nucleoid, $18 \mu\text{m}^3$) and obtained $x = 13.6$ and $y = 37.5$ – the *E. coli* B/r strains are indeed in the segregation regime II (Fig. 5). Thus, the replicating chromosomes could segregate purely driven by conformational entropy, and they will remain demixed ([Bates and Kleckner, 2005](#); [Jun and Mulder, 2006](#)).

B. Application to plasmid segregation.

Another important biological question concerns plasmid segregation in bacteria. Note that the size of typical plasmids is of order 10 kb, i.e., about < 1% of the total amount of DNA in the cell. Thus, the correlation length of the DNA in bacteria will not change because of the plasmids. In our phase diagram, this corresponds to changing both x and y values for the chromosome by a factor of $\sim 10^1$ (since $R_F \sim N^{3/5}$). This makes the plasmids enter the mixing regime V⁴ and they will distribute randomly inside the cell.

The quantitative reasoning above has broader implications for segregation strategies and copy-number control of plasmids ([Nordström and Gerdes, 2003](#)): (i) An *active* segregation mechanism, especially, for low-copy number plasmids, or (ii) “Random” segregation, i.e., without a protein-based segregation mechanism, plasmids may produce multiple copies so that, despite their small sizes, their chance of survival increases upon cell division. In random segregation, copy-number control is an interesting and important issue [See, for example, [Brenner and Tomizawa \(1991\)](#) and references therein].

REFERENCES

- Arnold, A., B. Borzorgui, D. Frenkel, B.-Y. Ha, and S. Jun, 2007, “Unexpected relaxation dynamics of a self-avoiding polymer in cylindrical confinement,” *J Chem Phys* **127**, 164903.
- Arnold, A., and S. Jun, 2007, “Timescale of entropic segregation of flexible polymers in confinement: Implications for chromosome segregation in filamentous bacteria,” *Phys Rev E* **76**, 031901.
- Bates, D., and N. Kleckner, 2005, “Chromosome and replisome dynamics in *E. coli*: loss of sister cohesion triggers global chromosome movement and mediates chromosome segregation,” *Cell* **121**, 899–911.
- Brenner, M., and J.-I. Tomizawa, 1991, “Quantitation of ColE1-encoded replication elements,” *Proc. Nat. Acad. Sci.* **88**, 405–409.
- Brochard, F., and P. G. de Gennes, 1979, “Conformation of molten polymers inside small pores,” *J. Phys. (Paris)* **40**, L399–L401.
- Cacciuto, A., and E. Luijten, 2006, “Self-avoiding flexible polymers under spherical confinement,” *Nano Lett* **6**, 901–905.
- Cates, M. E., and J. M. Deutsch, 1986, “Conjectures on the statistics of ring polymers,” *J Physique* **47**, 2121–2128.
- Daoud, M., and P. G. de Gennes, 1977, “Statistics of macromolecular solutions trapped in small pores,” *J. Phys. (Paris)* **38**, 85–93.
- Deng, S., R. A. Stein, and N. P. Higgins*, 2005, “Organization of supercoil domains and their reorganization by transcription,” *Mol Microbiol* **57**, 1511–1521.
- Grosberg, A. Y., P. G. Khalatur, and A. R. Khokhlova, 1982, “Polymeric coils with excluded volume in dilute solution: the invalidity of the model of impenetrable spheres and the influence of excluded volume on the rates of diffusion-controlled intermacromolecular reactions,” *Makromol. Chem., Rapid Commun.* **3**, 709–713.
- Grosberg, A. Y., and A. R. Khokhlov, 1994, *Statistical Physics of Macromolecules* (AIP Press).
- Jun, S., A. Arnold, and B.-Y. Ha, 2007, “Confined space and effective interactions of multiple self-avoiding chains,” *Phys Rev Lett* **98**, 128303.
- Jun, S., and B. Mulder, 2006, “Entropy-driven spatial organization of highly confined polymers: Lessons for the bacterial chromosome,” *Proc Nat Acad Sci USA* **103**, 12388–12393.
- Jun, S., D. Thirumalai, and B.-Y. Ha, 2008, “Compression and stretching of a self-avoiding chain in cylindrical nanopores,” *Phys Rev Lett* **101**, 138101.
- Jung, Y., S. Jun, and B.-Y. Ha, 2009, “A self-avoiding polymer trapped inside a cylindrical pore: Flory free energy and unexpected dynamics,” *Phys Rev E* **79**, 061912.

⁴ Note that, in principle, there are four determining parameters of our phase diagram, where the fourth parameter is the number of chains n . If we release the constraint imposed on n [e.g., $n = 2$ (chromosomes) and $n = 4$ (chromosomes + plasmids)], while keeping constant D and ξ_{bulk} , the two cells are connected by a diagonal line in the phase diagram because, then, R_F is the only additional variable (Fig. 5).

- Kubitschek, H. E., 1981, "Bilinear cell growth of *Escherichia coli*," *J Bacteriol* **148**, 730–733.
- Lal, J., S. K. Sinha, and L. Auvray, 1997, "Structure of Polymer Chains Confined in Vycor," *J. Phys. II (France)* **7**, 1597–1615.
- Marko, J. F., and E. D. Siggia, 1995, "Statistical mechanics of supercoiled DNA," *Phys Rev E* **52**, 2912–2938.
- Nordström, K., and K. Gerdes, 2003, "Clustering versus random segregation of plasmids lacking a partitioning function: a plasmid paradox?," *Plasmid* **50**, 95–101.
- Romantsov, T., I. Fishov, and O. Krichevsky, 2007, "Internal structure and dynamics of isolated *Escherichia coli* nucleoids assessed by fluorescence correlation spectroscopy," *Biophys J* **92**, 2875–2884.
- Sakaue, T., and E. Raphaël, 2006, "Polymer chains in confined spaces and flow-injection problems: some remarks," *Macromolecules* **39**, 2621–2628.
- Stavans, J., and A. Oppenheim, 2006, "DNA-protein interactions and bacterial chromosome architecture," *Phys Biol* **3**, R1–R10.
- Teraoka, I., and Y. Wang, 2004, "Computer simulation studies on overlapping polymer chains confined in narrow channels," *Polymer* **45**, 3835–3843.
- Woldringh, C. L., and T. Odijk, 1999, in *Organization of the Prokaryotic Genome*, edited by R. L. Charlebois (ASM Press, Washington, D.C.), 161–197.